Quantification of Brain Macrostates

Using Dynamical Nonstationarity of Physiological Time Series

Charles-Francois V. Latchoumane[1], *member IEEE*, Jaeseung Jeong[1], *member IEEE*

[1]Bio and Brain Engineering Department, Korea Advanced Institute of Science and Technology (KAIST), Daejeon, Republic of Korea, 305-701

The brain shows complex, nonstationarity temporal dynamics, with abrupt micro- and macrostate transitions during its information processing. Detecting and characterizing these transitions in dynamical states of the brain is a critical issue in the field of neuroscience and Psychiatry. In the current study, a novel method is proposed to quantify brain macrostates (e.g. sleep stages or cognitive states) from shifts of dynamical microstates or dynamical nonstationarity. A 'dynamical microstate' is a temporal unit of the information processing in the brain with fixed dynamical parameters and specific spatial distribution. In this proposed approach, a phase-space-based dynamical dissimilarity map (DDM) is used to detect transitions between dynamically stationary microstates in the time series, and Tsallis time-dependent entropy is applied to quantify dynamical patterns of transitions in the DDM. We demonstrate that the DDM successfully detects transitions between microstates of different temporal dynamics in the simulated physiological time series against high levels of noise. Based on the assumption of nonlinear, deterministic brain dynamics, we also demonstrate that dynamical nonstationarity analysis is useful to quantify brain macrostates (Sleep stages I, II, III, IV, and rapid eye movement (REM) sleep) from sleep EEGs with an overall accuracy of 77%. We suggest that dynamical nonstationarity is a useful tool to quantify macroscopic mental states (statistical integration) of the brain using dynamical transitions at the microscopic scale in physiological data.

***Index Terms*—dynamical nonstationarity, brain dynamics, microstates and macrostates, dissimilarity map, EEG**

I. Introduction

The brain exhibits complex, nonstationary temporal dynamics of information processing. Consequently, electroencephalograms (EEGs) show abrupt transitions between brain states at micro- and macroscopic time scales. Previous investigation on the temporal structure of brain dynamics using nonlinear dynamical methods, as well as linear methods, has been performed to examine normal and pathological states. Particularly, the application of these nonlinear methods to EEGs in patients with neurological and psychiatric disorders has proven to be effective for diagnosing various brain diseases and for quantifying the progress of the diseases (for review, see [1, 2]).

Several previous studies support the assumption of spatio-temporal dynamics of the brain by demonstrating the presence of electrical microstates in the brain and their associations with cognitive states [3-5] or pathological states like seizure [6-9]. The brain microstate is defined as a temporal unit of neural assembles in specific spatial distribution that coordinates for information processing of the brain, expressed as the existence of potential extrema, phase synchronization of specific frequency bands, and so forth [3-5, 10]. In the context of dynamical nonstationarity, brain microstates exhibiting stationary dynamical properties are by extension called 'brain dynamical microstates.' Moreover, weak statistical parameters of time series (i.e. low-order statistics) generated by nonlinear deterministic systems including mean, variance, and power spectrum may significantly vary over time (statistical nonstationarity), despite all the parameters in the dynamical process remaining constant (dynamical stationarity). This indicates that statistical stationarity of brain microstates does not imply their dynamical stationarity. Thus, dynamically stationary microstates are different from its statistical counterpart and may imply a more general definition for mental-state units [1].

Le Van Quyen et al. [9] and Dikanev et al. [6] applied the dynamical nonstationarity method (i.e. spatio-temporal structure analysis of EEGs segmented into dynamical microstates) to investigate the potential predictability of seizures in epileptic patients. Similarly, the classification and clustering of the time series using nonlinear measures [6, 11] or the combination of linear and nonlinear methods for EEG recordings [12] showed that nonlinear measures are complementary to linear ones and have a potential to distinguish dynamical states and possibly to characterize temporal alternations in mental states (e.g. sleep stages or seizure onset). However, we note that nonlinear determinism of EEGs is controversial [1], which limits the application of dynamical nonstationarity.

It was demonstrated the presence of weak nonlinear determinism in all sleep stages [13] and showed that it was particularly pronounced in deeper sleep stages (i.e. slow wave sleep (SWS) stages) [14, 15]. More importantly, the long-range temporal correlations and multi-scale nature of electrophysiological activity in the brain [16] suggest nonlinear brain dynamics at the fast temporal scale and their statistical integration at the slower scale [17]. Hence, the temporal scale of consideration appears to be crucial for understanding the cause of nonlinearity and the underlying mechanism of information processing in the brain, as

Manuscript received January 14, 2009. Corresponding author: J. Jeong (e-mail: jsjeong@kaist.ac.kr).
Digital Object Identifier inserted by IEEE

demonstrated for sleep EEGs [18]. Previous studies using nonlinear methods integrated dynamical information over segments of physiological time series (e.g. EEGs) ranging from 16s to over several minutes in length [12, 15, 18], and directly attempted to characterize mental states based on its dynamical properties. However, it is supported that dynamical microstates could be understood as temporal units (i.e. hundreds of milliseconds to tens of seconds) of information processing [3, 5, 10, 18], forming cyclic and alternative patterns of brain dynamics [19].

In this study, we propose a method optimized for automatic quantification of mental states based on alternating patterns of dynamical microstates. The aim of this study is to investigate the possible multi-nature (dynamical and statistical) and multi-scale (micro- and macroscale) coding of EEGs using the novel approach of dynamical nonstationarity. The structure of this article is organized as follows: in Section II, the methodology for macrostate quantification using dynamical nonstationarity is presented; in Section III, the applicability of dynamical nonstationarity method to a simulated physiological time series with additional noise for detecting transitions between dynamical states is demonstrated; Section IV presents the results for the quantification of sleep stages using sleep EEGs. We suggest that dynamical nonstationarity is a potential tool for characterization of mental states and for analysis of various abnormal EEGs recorded from neuropsychiatric disorders. This method may provide with insight into a possible coding of brain information processing from its inner dynamics.

II. METHOD

The core idea of this method is as follows: A time series is divided into short segments and their dynamics are reconstructed in the multi-dimensional phase space using Takens' embedding theorem. A limit set of trajectories in the phase space is called the attractor reflecting temporal dynamics of the time series, and thus is compared between each of segments using the phase-space dissimilarity measure (PSDM). The dynamical dissimilarity calculated between a given set of reference and test segments of the time series results in the dynamical dissimilarity map (DDM), which is used to characterize the transitions between dynamical microstates of the brain (i.e. local dynamics). Sleep stages are macrostates of the brain (i.e. global brain dynamics) that consist of specific combinations of dynamical microstates. Thus, Tsallis time-dependent entropy is estimated to characterize the temporal changes in the dynamical pattern of the DDM. The calculated Tsallis entropy values are used to train a linear classifier to detect the transitions between macrostates of the brain. A schematic diagram of this method is illustrated in Fig. 1.

FIG 1 HERE

A. Estimation of Dynamical Dissimilarity

For an one-dimensional time series (e.g. an EEG time series), a multi-dimensional topological geometry is reconstructed within a reference space, which is called the 'phase space' [20]. The phase space representation of the given time series is the topological transposition of the associated system dynamics along its generalized coordinate, i.e. the degree of freedom. The attractor is the limit set of points or trajectories to which a dissipative, dynamical system evolves asymptotically in the reconstructed phase space. The attractor captures the underlying dynamics of the time series in the reconstructed phase space. For deterministic systems, changes in values of parameters can be detected in the equations that govern the behavior of the system. Several methods have been developed to detect dynamical changes within and between segments of a time series, including recurrence plot methods [21, 22], statistical analysis of a reconstructed phase space [23], plotting the space time index [24], use of nonlinear cross prediction [25], and phase-space dissimilarity measurement [7, 8, 26].

For this study, a dynamical dissimilarity measure called the phase-space dissimilarity measure (PSDM) was chosen to quantify the brain microstates from physiological time series. The PSDM compares the occupation distributions of the attractors for two segments of the time series. The PSDM has proven to be effective in detecting alternations in dynamics in noisy, physiological time series, as demonstrated in the anticipation of onset of seizures in epileptic patients using EEGs [7, 8, 26]. In this study the non-connected PSDM based on the χ^2 distance was used.

B. Dynamical Dissimilarity Map

Considering an automated approach, a priori access to the number, duration, and location of different dynamically stationary segments is not available. As an alternative to the binary decision approach (i.e. detection-or-not based on a threshold), a dynamical dissimilarity map (DDM) was applied to allow the identification of transitions between several different dynamical states and their evolution over time. For the time series $x(t)$ of N data points, the DDM is the matrix $R_{ref} \times N_{test}$ that contains the dissimilarity values calculated from the PSDM between each of the non-redundant reference segments (R_{ref}) and each of the test segments (N_{test}). For each test segment, the R_{ref} dissimilarity values provide an identification vector based on the dynamics contained in the reference segments.

First, we assume N_{ref} contiguous, non-overlapping reference segments of length W are chosen across the entire, original time series $x(t)$; thus, $N_{ref} \sim N/W$. These reference segments cover the distribution of the dynamical signature contained in the original time series. In this analysis, we assume that an EEG time series has a finite number of distinct dynamical states with finite durations, and consequently the mapping of the dynamical similarity contains distinct temporal patterns through the variations of the inter-dynamical dissimilarity (i.e. local dynamics). Among the N_{ref} reference segments, several segments might contain redundant information about the different dynamics present in the time series.

Second, test segments are chosen, each with a length of W points and an overlap of OV data points to span the entire time series, $x(t)$. This choice yields a total number of test segments, $N_{test} = N/(W-OV)$. If $OV = 0$, the set of reference and test

segments are identical. The length W should be sufficiently large to calculate the PSDM and should contain the least number of different dynamical microstates so as not to mask the patterns of the dynamical microstate. The resolution W - OV is related to the duration of the shortest dynamical microstate. The proper values for W and OV should be determined by the consideration of the trade-off between the temporal resolution and the accuracy in the dissimilarity estimation (i.e. estimation of state space occupation distribution).

Third, a K-clustering method was used to form $K = R_{ref}$ clusters (see Appendix-1) out of the N_{ref} reference segments. The cluster centers designate the R_{ref} non-redundant reference segments. Thus, the DDM originally $N_{ref} \times N_{test}$ is reduced to $R_{ref} \times N_{test}$.

C. Time-dependent Entropy for Macrostate Quantification

The ultimate goal of this study is to provide a quantification of macrostates from their underlying dynamical nonstationarity. In Section III, we show that the DDM contains all relevant information for the characterization and identification of dynamical microstates. To characterize macrostates of the brain, such as sleep stages and certain cognitive states, we should assume that macrostates exhibit specific patterns of brain microstates. The shifting patterns of microstates are directly reflected into the DDM, which is quantified by time-dependent Tsallis entropy. After normalization into M bins, each of the R_{ref} rows of the DDM exhibits a sequence of integer numbers. Transitions between different dynamics are represented as changes in symbolic sequences with long-term correlations, which can be described using an extensive entropy, the Tsallis entropy [27, 28]. The Tsallis entropy is a generalization of the standard Boltzmann-Gibbs entropy that accounts for the nonextensive degree of irregularity and complexity for the system under study through an entropic index q [28], and is calculated as follows:

$$TDE = \frac{1-\sum_{i=1}^{M} p_i^{\,q}}{q-1}, \qquad (1)$$

where M is the total number of microscopic possibilities of the system (i.e. the number of bins) and p_i the probability of the i-th microscopic state. Each of the R_{ref} row elements of the DDM (i.e. $R_{ref} \times N_{test}$) is divided into windows of w_{TDE} data points and ov_{TDE} overlapping data points. The time-dependent version of Tsallis entropy (TDE) [29] is estimated as the Tsallis entropy on each of the windows of a row of the DDM. To describe the temporal evolution of dynamical dissimilarity patterns with an emphasis on frequent occurrence [29, 30], a fixed partition design and an entropic index of q = 1.5 were applied.

D. Parameter Estimation for Phase Space Reconstruction

The attractor is reconstructed in phase space from the observed sequence $x(t)$ by plotting delay vectors using what is referred to as an embedding procedure. Here, the delay vectors $y(t) = [x(t), x(t+\tau), ..., x(t+(d-1)\tau]$ are constructed from an observed single time series $x(t)$, where τ is the time delay and d is the embedding dimension, to unfold the projection back to a multivariate phase space that is a valid representation of the original deterministic dynamical system; the attractor thus reconstructed is topologically equivalent to the original dynamical system under certain general conditions [20].

To estimate the proper embedding parameters, embedding dimension and time delay, the method based on Kozachenko-Leonenko (KL) differential entropy is used [31, 32]. This method is shown to provide the optimal pair of embedding dimension and time delays (d, τ) for phase-space reconstruction. The Kozachenko-Leonenko (KL) estimate of the differential entropy of the data x is given by:

$$H(x) = \sum_{i=1}^{W} \ln(W \rho_i) + \ln(2) + C_E, \qquad (2)$$

where W is the number of samples in the data $\boldsymbol{x}$, ρ_i is the Euclidian distance of the j-th delay vector of the data x to its nearest neighbor and C_E ($\approx$ 0.5772) is the Euler constant. Then, for given pair of embedding parameters (d, τ), H($\boldsymbol{x}$, d, τ) is the differential entropy estimate for the delay vector version of the time series $\boldsymbol{x}$. The optimal values of embedding parameters are obtained from the minimum of the entropy ratio (ER):

$$ER(d,\tau) = \frac{H(x,d,\tau)}{\left\langle H(x_s,d,\tau)\right\rangle_s}\left(1+\frac{d\ln W}{W}\right), \qquad (3)$$

where $< >_s$ denotes the mean over s surrogate data for the original time series $\boldsymbol{x}$, $\boldsymbol{x_s}$. In Eq. 3, the ratio of differential entropy by the mean differential entropy over the surrogate data is weighted by the "minimum description length" (MDL) to penalize for higher embedding dimension. For ER estimation, it is necessary to use surrogate data for the original time series [33]. The surrogate data were generated herein by first computing the Fourier transforms of the original signals, randomizing the Fourier phase while preserving the moduli, and then performing inverse Fourier transform. Surrogate data have amplitude spectra identical to the original signals, but possible temporal correlations are destroyed. The systematic test against the surrogate data increases the advantages of this method against noise, dimensionality, and autocorrelation effects. For each time series, an average value of the pair (d, τ) was estimated over the N_{ref} reference segments.

For the density distribution in the phase space, different values of binning S were tested in the range [5, 25] to address several different levels of noise present in the time series and then integrated in the dynamical dissimilarity mapping. We used an uniform binning following $s(i) = INT\left[(S(x(i)-x_{\min})/(x_{\max}-x_{\min})\right]$, where INT rounds a decimal value down to the next lower integer, and x_{min} and x_{max} are the minimum and maximum value of the given time series, respectively. It was empirically observed that S within the range [5, 10] produces the highest contrast between the different dynamics.

III. Dynamical Microstate Detection

In this section, the DDM calculated from the PSDM is tested for distinguishing different dynamical microstates from a time series with noise. An artificial physiological

nonstationary time series was generated using the Mackey-Glass system [34, 35] with different levels of Gaussian noise, and the DDMs of these simulated time series were computed. A clustering method was applied to the DDM to identify the dynamical microstate (see appendix), and then a true rate of microstate identification was obtained. The quantification of brain macrostates is not considered in this section.

A set of stationary time series were generated from the delayed differential equation using the 4th order Runge-Kutta integration method:

$$\frac{dx(t)}{dt} = y_i(t) = -0.1x(t) + \frac{0.2x(t-t_i)}{1+x(t-t_i)^{10}}. \qquad (4)$$

Complex stationary time series were obtained from the mixed patches of the time series having three primary stationary regimes of the Mackey-Glass system (t_1 = 17, t_2 = 23, and t_3 = 30) as follows:

$$\frac{dx(t)}{dt} = \sum_{i=1}^{3} \alpha_i y_i(t). \qquad (5)$$

The coefficient α_i denotes the weight corresponding to the stationary time series generated using t_i, i = 1, 2 and 3, and $\alpha_1 + \alpha_2 + \alpha_3 = 1$. Each mixed patch of the time series is designated by the value of each of the three weights, $Coef = (\alpha_1, \alpha_2, \alpha_3)$. Dynamically nonstationary time series were generated with an exponential drift of duration D_{trans} between stationary time series of different weight values. Transitions from the stationary time series $A(t)$ to another stationary time series $B(t)$ were detected from t_0 to $t_0 + D_{trans}$ below:

$$a(t) = \exp(-4t / D_{trans}), \qquad (6)$$

$$x(t) = a(t-t_0)A(t) + (1-a(t-t_0))B(t). \qquad (7)$$

Finally, the Gaussian noise was added to this simulated times series with the same mean as the original time series and with the standard deviation (SD) equal to several different percentages of the SD of the original time series.

In Fig. 2, the time series (Fig.2(a), solid line) exhibited successive transitions between the consecutive patches of the stationary time series with different coefficients $Coef1$ = (1, 0, 0), $Coef2$ = (0, 1, 0), $Coef3$ = (0.2, 0.3, 0.5), and $Coef4$ = (0.1, 0.6, 0.3), and each with a duration of 1,000 data points (Fig. 2(c)) after the onset of the transition (D_{trans} = 100 points; Fig. 2(c)) repeated twice in a cycle (i.e. seven transitions). The partition of the original simulated time series (Fig. 2(d)) was obtained using K-affinity propagation (see appendix-2), an unsupervised method attempting to recognize the number of clusters K, with K = 4 applied on the dynamical dissimilarity matrix calculated with W = 400, OV = 350, S = 5, d = 2 and τ =23 (Fig. 2(b)). The proposed choice of parameters for W, OV and S were obtained after optimization based on the true rate identification of the microstate and for K = 4 different microstates and no additional noise. Particularly, it was observed that given the duration of a microstate (i.e. 1,000 data points), $W >> S^d$, $W < 700$ and $(W - OV) < 50$ were critical criterion to distinguish the dynamical microstates and their transitions (i.e. total true rate > 80 %). Best results were found for the pairs (W, OV) = (350, 330) and (400, 350). Fig. 2 (c and d) shows that this algorithm successfully detected the presence of four different dynamics and their correct onset and offset times. This result was compared with the original dynamical states with additional Gaussian noise (20% SD of the time series as its SD) (Fig. 2(c)).

FIG 2 HERE

To confirm the robustness of this method against noise, the performance of the method was evaluated for nonstationary a Mackey-Glass time series exhibiting transitions between two, three, and four different dynamical states with an increasing SD of noise over 100 trials. Fig. 3 shows the performance (the true positive rate of detection for transitions between different dynamical states) of the K-affinity propagation with K set to the number of dynamics known to be present in the time series (K = 2, 3, and 4). The time series had two (i.e. Coef1, Coef2 and K set to 2 for the K-affinity propagation), three (i.e. Coef1, Coef2, and Coef3, and K set to 3 for the K-affinity propagation), and four (i.e. Coef1, Coef2, Coef3, and Coef4, and K set to 4 for the K-affinity propagation) different dynamical states (i.e. 7 transitions of length D_{trans} = 100 data points for a total length of N = 9,000 data points). It was found that the DDM calculated from the PSDM successfully characterized the presence of two, three and four different dynamics, resulting in clustering accuracy over of 80% against several different levels of noise, as shown in Fig. 3. The presence of dynamical transitions yielded approximately 4% error. The performance in distinguishing different dynamics showed about 72% or larger of correct identification rates even for the time series with 70% SD of additional Gaussian noise.

FIG 3 HERE

IV. Results

We investigated whether the proposed method can quantify macrostates of the brain from physiological datasets or not. The dynamical nonstationarity analysis was performed to quantify dynamical patterns of sleep EEGs. Sleep stages are typical examples of macrostates of the brain, and automatic sleep staging is not only clinically significant but also has been used as a benchmark to assess the possibility of physiological or clinical application for engineering methods [34, 36]. We applied the time-dependent Tsallis entropy to the DDM ($R_{ref} \times N_{test,}$ i.e. R_{ref} features), and investigated whether or not the entropic coding of the dynamical EEG patterns is associated with sleep stages manually determined by clinicians. A multivariate discriminant classifier, one of the simplest probabilistic classifiers based on linear discriminant analysis, was trained to distinguish sleep stages.

A. Subjects & EEGs

EEG recordings were obtained from 17 subjects in the MIT-BIH polysomnographic database [37, 38] (which were available at http://www.physionet.org/physiobank/database/slpdb/). The manual segmentation information by clinicians of sleep stages at intervals of 30 sec was also provided at the website. Five subjects (slp03, slp14, slp41, slp45 and slp66) with missing data or high frequency transition between sleep stages (i.e. too considerable nonstationarity of macrostates) were discarded to

ensure more stability in the detection of macrostates. The 12 subjects were selected to exhibit four different sleep stages such as sleep stages I and II, slow wave sleep (SWS; combining stages III and IV), and Rapid Eye Movement (REM) sleep. The EEG recordings were sampled at 250 Hz and recorded from either electrodes C4-A1, O2-A1 or C3-O1, and with duration ranging from 120 min to 390 min. As suggested for the same MIT-BIH database [39], ECG artifacts were removed from each EEG recording using Independent Component Analysis (ICA) from EEGLAB 6.01b on Matlab® [40] based on the ECG and EEG channels. Low frequency artifacts, including eye blinking and other movement artifacts, were removed using a zero-phase quadratic filter with a total window length of 125 data points, corresponding to a cutoff frequency of 2Hz [26].

B. Classification of Sleep Stages

Using the phase-space dissimilarity measure (PSDM) and the time-dependent entropy (TDE), respectively, the local and global changes in brain dynamics within sleep EEGs were estimated. For the calculation of the DDM using the PSDM, W = 2,000 data points (i.e. 8 sec of recording) and OV = 1,900 points with an interval of 100 points (400 msec of resolution) were chosen. The window size W was chosen to be sufficiently large to produce a reliable estimate of the distribution being considered (i.e. following the criterion $W >> S^d$, with (d, τ) estimated as (2, 17) and S = 5) and suitable for the estimation of a microstate of duration lower than 15 sec. To estimate the TDE for each row of the DDM, a window size w_{TDE} = 650 and overlapping ov_{TDE} = 645 were chosen. The parameters w_{TDE}, ov_{TDE} and R_{ref} were obtained after varying each parameter with the others fixed and based on the true detection rate over the subjects slp01a, slp02a and slp14 (i.e. subjects exhibiting all sleep stages including wake stage and movement time). For fixed $(w_{TDE} - ov_{TDE})$, there was no substantial changes for w_{TDE} as low as 300 points [41]. This method provided entropy values for each R_{ref} row of the DDM at an interval of $(W - OV)$ x $(w_{TDE} - ov_{TDE})$ = (2,000 – 1,900) x (650 - 645) = 500 data points, which eventually correspond to one value every two seconds. 15 values of entropy per current sleep stage of 30 sec were then obtained, and they were then compared with the sleep stage information determined manually by clinicians.

We found that the classification accuracy of this method for sleep staging using R_{ref} = 20 (i.e. 20 features for the classification) was 77.0% (range: 66.0-94.3%) for 12 subjects based on the true rate of sleep stage classification (Table 1). The average accuracy for the classification of SWS (sensitivity: 88.8%; specificity: 94.9%) and REM sleep (sensitivity: 82.4%; specificity: 95.9%) was higher than 80.0%. The classification of sleep stage II (sensitivity: 76.2%; specificity: 83.7%) had the least consistency, with a sensitivity ranging from 57.3% to 100%. Most of the misclassifications were observed between sleep stages I and II when dealing with all stages.

TABLE 1 HERE

C. Principal Component Analysis of Entropy Features

The R_{ref} features of the entropy-transformed DDM are possibly used directly in a classifier, but it would be impractical given their number (R_{ref} = 20 for sleep-stage classification) and their individual meaning (each selected reference should encode for a single microstate pattern). Hence, a principal component analysis (PCA) was applied to the R_{ref} vectors encoding for sleep stages to obtain a more informative and uncorrelated perspective on the classification features. The PCA implies the orthogonalization of the R_{ref} vectors, resulting in uncorrelated principal components ordered from the largest to the lowest amount of explained variance of the original data [42].

TABLE 2 HERE

We found that, for all subjects, maximally six principal components (range: 2-6) were sufficient to recover 99% of the original variance. In Table 2, the classification using principal components covering 99% of the explained variance showed decreased accuracy (sensitivity) down to 80% for comparisons including sleep stages I and II, as compared with the classification using the original entropy features. The classification of sleep stages I and II obtained the worst accuracy (sensitivity: 78.7%; specificity: 86.2%), dramatically dropping after application of PCA to the entropy features (sensitivity: 67.5%; specificity: 75.3%). The classification accuracy of sleep stages SWS and REM was left relatively unchanged after PCA, with an accuracy decrease for the SWS stage of less than 1.2%.

V. Conclusion

Since nonstationarity is an intrinsic property in physiological and clinical recordings from biological systems, it is critical to understand their properties and possible roles in order to describe and control the system. We have considered biological systems as stationary and applied statistical or dynamical methods to the systems, which might lead to spurious results. Furthermore, nonstationarity in a time series has been defined and investigated based on statistical properties of the time series. In this study, we propose that dynamical nonstationarity of EEG recordings is associated with brain macrostates during the information processing of the brain. Although the PSDM is relatively sensitive to noise and artifacts, we demonstrate that the DDM reliably detects transitions between different dynamical states with an accuracy of about 80% or higher against high levels of Gaussian noise (SD_{EEG}/SD_{Noise} smaller than 30%). This robustness of the method against noise suggests its possible application to physiological or clinical time series. Moreover, we suggest that this proposed method is useful for determining transitions between different brain macrostates (e.g. sleep stages from artifact-free sleep EEG recordings) based on specific pattens of brain microstates with prominent accuracy.

Although previous studies on sleep staging techniques have yielded a classification accuracy ranging between 85% - 91% [43], lower performance accuracy (about 61%) than that resulting from the method proposed here has been reported for

the same MIT-BIH database from previous studies, such as from recurrence quantification analysis [39]. Moreover, the existing automatic sleep-staging methods with high performance are often based on sophisticated experts [34, 43, 44] and nonlinear classifiers [45]. Thus, these methods may suffer from database bias and low generalization, and are not directly comparable with the present method (i.e. feature extraction and linear classification). Even when the proper linear and nonlinear features are selected and/or combined, classification accuracy often saturates around 80% [12, 46]. In addition to reasonable classification accuracy (about 77%), the method proposed here applies to estimate dynamical nonstationarity, an intrinsic property of EEG recordings, as a feature to quantify and differentiate sleep stages (i.e. macrostates). We suggest from this preliminary finding that dynamical nonstationarity is useful for describing complex temporal dynamics of the brain using physiological time series like EEGs. Particularly, the duration and transition timings of dynamically stationary states in physiological recordings can be quantified using this method.

The assumption of this method that EEG recordings are governed by nonlinear deterministic processes [47, 48] rather than stochastic processes [49, 50] is still controversial. EEGs have been found to have deterministic, chaotic characteristics, including finite values of the correlation dimension and positive Lyapunov exponents, but stochastic properties of EEGs have also been reported (for review, see [1, 2]). Nonlinear dynamical properties of EEGs were mostly found in deep sleep stages (i.e. sleep stages III and IV or slow wave sleep, SWS) using nonlinear dynamical measures including the correlation dimension [14] and coarse-graining spectral analysis method [15]. In these studies, nonlinear measurement had a higher classification performance for the SWS stage and stage II, while the other study demonstrated better performance of nonlinear measurement over spectral analysis for distinguishing between stage I and stage II [12]. The PCA analysis of entropy features revealed that the SWS and REM stages are best differentiated using the dynamical nonstationarity method (i.e. sensitivity > 92% before and after PCA). The entropy quantification of sleep stages I and II appeared to be less reliable, as the principal components cannot provide the stable discriminative power. In general, the application of nonlinear analysis methods to quantification of stages I, II and REM sleep have produced lowered performance; however, nonlinear measures that cope with nonstationarity, such as detrended fluctuation analysis method [51, 52] and dynamical nonstationarity method, might capture an instantaneous dynamical structure with less constraints on 'nonlinearity' hypothesis. Although the present study supports the presence of the nonstationary, nonlinear dynamical nature of sleep EEGs in the multi temporal scales [53], finding it particularly pronounced in the SWS and REM stages, the assumption of dynamical nonstationarity should be used with extreme caution.

In this method, proper window size is critical for reliably detecting brain microstates in EEG recordings. The resolution of 400msec was used for the estimation of the DDM map and a couple of seconds were used for the estimation of the entropic pattern of the DDM. Previous studies reported the existence of microstates with the duration of 100 msec or longer based on the global field potential extrema and spatial distributions [3, 5], or phase pattern dynamics of alpha waves using Hilbert transform [10]. They hypothesize decomposition of temporal brain dynamics into microstates using event-related potentials or alpha-band EEGs. In addition, both the PSDM and the Tsallis entropy are statistical measures that require a large number of data points to reliably estimate their distribution functions. The current method used W = 2,000 data points to produce reliable values in detecting dynamical shifts [7, 8]. However, it was important to keep the W value small enough to not contain too many different dynamics to detect microstates in the brain. The results of this study are consistent with previous findings on the duration of microstates. The results of this study suggest that, as well as the duration of microstates themselves, temporal patterns of microstates (i.e. dynamically stationary states) and their transitions should be considered to understand possibly associated mental states in a higher scale [10].

It is important to note that the epochs marked by clinicians and with movement time were not utilized here, while the epochs marked with single limb movement associated or with apnea were used. The stages I (22.6% of epochs) and II (57.1% of epochs) were the dominant stages in this database, also marked with a large amount of apnea or single limb movement periods: 71.1% of sleep stage I and 62.1% of sleep stage II. Thus, the effects of movement and apnea on the dynamical nonstationarity could explain the reduced inconsistency in classification of stage I (overall accuracy: 72.3%; range: 57.7-100%) and II (overall accuracy: 76.2%; range: 57.3-100%) and should be investigated in future to improve the accuracy of this proposed method for sleep-staging. Moreover, in addition to different electrode set-up, the presence of marked periods of apnea and single limb movement increased the inter-subject variability and limited the investigation in terms of determining the universality of this method.

In summary, a novel method to quantify brain macrostates from the dynamical nonstationarity of EEG recordings is proposed in this study. We demonstrate that this method is useful for detecting transitions between different temporal dynamical states in a time series with high levels of noise. We suggest the possibility of sleep staging from the temporal quantification of dynamical nonstationarity in sleep EEG recordings, with an overall accuracy of 77%. There have been several studies reporting abnormal temporal dynamics of the brain and pathological transitions between brain microstates, such as seizures, Attention-Deficit Hyperactivity disorder (ADHD), Alzheimer's disease, and Schizophrenia [6, 8, 54-56]. Whether this method is helpful for diagnosing and quantifying the severity of such diseases or not should be further investigated.

APPENDIX

The affinity propagation is a recently developed clustering

algorithm which iteratively determines clusters and their centers (i.e. centroids) using cumulated and propagating "affinity" between pairs of data points in a time series [57]. Conventional K-clustering methods iterate from randomly chosen centroids (i.e. converge well only if the initial centroids are close to the good solution). The affinity propagation rather attributes weights or "preference" values which, if chosen sufficiently large, bias a point to be centroid. The preference is usually set to a common value for all points (i.e. all points are potential centroids), and the value of this common reference governs the final number of clusters. The K-cluster algorithm derived from the affinity propagation, which is called K-affinity propagation, estimates the optimal starting preference value to obtain the user-defined number of clusters *K* within a tolerance given in percentage.

In this study, the K-affinity propagation was used for the two following purposes:

1) Dimension reduction using K-affinity propagation: The dynamical dissimilarity map (DDM) is a matrix formed by N_{test} vectors of N_{ref} features. The N_{ref} features are obtained from the dissimilarity between the reference segments and the current test segment. The selection of reference was originally made without a priori knowledge of their intrinsic dynamics, leading to the selection of segments with redundant dynamics. The K-clustering of the reference segment can reduce the number of feature for classification to non-redundant dynamics (pruning), however not uncorrelated, and is based on an optimizable, user-defined parameter $K = R_{ref}$.

2) Identification of microstate in simulated time series: In Section III, the K-affinity is directly applied to temporal clustering of the DDM (i.e. clustering of test segments). The purpose is to demonstrate that the DDM contains reliable features for the identification of different dynamical microstates, which is assessed using an unsupervised method (clustering).

ACKNOWLEDGMENT

The authors would like to thank Drs. Lee M. Hively (Oak Ridge National Laboratory, USA) and Thomas Schreiber (Max Planck Institute for physics of Complex Systems, Germany) for their valuable comments on this method. This work was supported by a Korea Science and Engineering Foundation (KOSEF) grant funded by the Korean government (MOST) (No. R01-2007-000-21094-0 and No. M10644000013-06N4400-01310). The authors thank the Ministry of Information and Technology of South Korea, the Institute for Information and Technology Advancement (IITA) and the Chung MoonSoul Research center at KAIST for their financial support.

REFERENCES

[1] C. J. Stam, "Nonlinear Dynamical Analysis of EEG and MEG: Review of an Emerging Field," *Clinical Neurophysiology,* vol. 116, pp. 2266-2301, 2005.

[2] J. Jeong, "EEG Dynamics in Patients with Alzheimer's Disease," *Clin Neurophysiol,* vol. 115, pp. 1490-505, 2004.

[3] D. Lehmann, W. K. Strik, B. Henggeler, T. Koenig, and M. Koukkou, "Brain Electric Microstates and Momentary Conscious Mind States as Building Blocks of Spontaneous Thinking: I. Visual Imagery and Abstract Thoughts," *Int J Psychophysiol,* vol. 29, pp. 1-11, 1998.

[4] J. Wackermann, D. Lehmann, C. M. Michel, and W. K. Strik, "Adaptive Segmentation of Spontaneous EEG Map Series into Spatially Defined Microstates," *Int J Psychophysiol,* vol. 14, pp. 269-83, 1993.

[5] R. D. Pascual-Marqui, C. M. Michel, and D. Lehmann, "Segmentation of Brain Electrical Activity into Microstates: Modele Estimation and Validation," *Biomedical Engineering, IEEE Transactions on,* vol. 42, pp. 658-665, 1995.

[6] T. Dikanev, D. Smirnov, R. Wennberg, J. L. Velazquez, and B. Bezruchko, "EEG Nonstationarity during Intracranially Recorded Seizures: Statistical and Dynamical Analysis," *Clin Neurophysiol,* vol. 116, pp. 1796-807, Aug 2005.

[7] L. M. Hively and V. A. Protopopescu, "Channel-consistent Forewarning of Epileptic Events from Scalp EEG," *Biomedical Engineering, IEEE Transactions on,* vol. 50, pp. 584-593, 2003.

[8] L. M. Hively, V. A. Protopopescu, and N. B. Munro, "Enhancements in Epilepsy Forewarning via Phase-Space Dissimilarity," *Journal of Clinical Neurophysiology,* vol. 22, p. 402, 2005.

[9] M. Le Van Quyen, J. Martinerie, V. Navarro, P. Boon, M. D'Have, C. Adam, B. Renault, F. Varela, and M. Baulac, "Anticipation of Epileptic Seizures from Standard EEG Recordings," *Lancet,* vol. 357, pp. 183-8, Jan 20 2001.

[10] J. Ito, A. R. Nikolaev, and C. Leeuwen, "Dynamics of Spontaneous Transitions between Global Brain States," *Human Brain Mapping,* vol. 28, p. 904, 2007.

[11] T. Schreiber and A. Schmitz, "Classification of Time Series Data with Nonlinear Similarity Measures," *Physical Review Letters,* vol. 79, pp. 1475-1478, 1997.

[12] J. Fell, J. Roschke, K. Mann, and C. Schaffner, "Discrimination of Sleep Stages: a Comparison between Spectral and Nonlinear EEG Measures," *Electroencephalography and Clinical Neurophysiology,* vol. 98, pp. 401-410, 1996.

[13] Y. Shen, E. Olbrich, P. Achermann, and P. F. Meier, "Dimensional complexity and spectral properties of the human sleep EEG," *Clinical Neurophysiology,* vol. 114, pp. 199-209, 2003.

[14] P. Achermann, R. Hartmann, A. Gunzinger, W. Guggenbuh, and A. A. Borbely, "Correlation dimension of the human sleep electroencephalogram: cyclic changes in the course of the night," *European Journal of Neuroscience,* vol. 6, pp. 497-500, 1994.

[15] E. Pereda, A. Gamundi, R. Rial, and J. Gonzalez, "Non-linear Behaviour of Human EEG: Fractal Exponent versus Correlation Dimension in Awake and Sleep Stages," *Neuroscience Letters,* vol. 250, pp. 91-94, 1998.

[16] K. Linkenkaer-Hansen, V. V. Nikouline, J. M. Palva, and R. J. Ilmoniemi, "Long-Range Temporal Correlations and Scaling Behavior in Human Brain Oscillations," *Journal of Neuroscience,* vol. 21, p. 1370, 2001.

[17] M. Le Van Quyen, "Disentangling the Dynamic Core: a Research Program for a Neurodynamics at the Large Scale," *Biological Research,* vol. 36, pp. 67-88, 2003.

[18] E. Olbrich, P. Achermann, and P. F. Meier, "Dynamics of human sleep EEG," *Neurocomputing,* vol. 52, pp. 857-862, 2003.

[19] R. Ferri, L. Parrino, A. Smerieri, M. G. Terzano, M. Elia, S. A. Musumeci, S. Pettinato, and C. J. Stam, "Non-linear EEG Measures during Sleep: Effects of the Different Sleep Stages and Cyclic Alternating Pattern," *International Journal of Psychophysiology,* vol. 43, pp. 273-286, 2002.

[20] F. Taken, "Detecting Strange Attractors in Turbulence," *Lecture Notes in Mathematics, ed DA Rand & LS Young,* 1981.

[21] C. L. Webber and J. P. Zbilut, "Dynamical Assessment of Physiological Systems and States using Recurrence Plot Strategies," *Journal of Applied Physiology,* vol. 76, pp. 965-973, 1994.

[22] A. Facchini, H. Kantz, and E. Tiezzi, "Recurrence Plot Analysis of Nonstationary Data: The Understanding of Curved Patterns," *Physical Review E,* vol. 72, p. 21915, 2005.

[23] M. B. Kennel, "Statistical Test for Dynamical Nonstationarity in Observed Time Series Data," *Physical Review E,* vol. 56, pp. 316-321, 1997.

[24] D. Yu, W. Lu, and R. G. Harrison, "Space Time-index Plots for Probing Dynamical Nonstationarity," *Physics Letters A,* vol. 250, pp. 323-327, 1998.

[25] T. Schreiber, "Detecting and Analyzing Nonstationarity in a Time Series Using Nonlinear Cross Predictions," *Physical Review Letters,* vol. 78, pp. 843-846, 1997.

[26] V. A. Protopopescu, L. M. Hively, and P. C. Gailey, "Epileptic Event Forewarning From Scalp EEG," *Journal of Clinical Neurophysiology,* vol. 18, p. 223, 2001.
[27] M. Buiatti, P. Grigolini, and L. Palatella, "A Non-extensive Approach to the Entropy of Symbolic Sequences," *indicators,* vol. 3, p. 7, 2008.
[28] C. Tsallis, "Nonextensive Statistics: Theoretical, Experimental and Computational Evidences and Connections," *Brazilian Journal of Physics,* vol. 29, pp. 1-35, 1999.
[29] N. V. Thakor and S. Tong, "Advance in Quantitative Electroencephalogram Analysis Methods," *Annual Review of Biomedical Engineering,* vol. 6, pp. 453-495, 2004.
[30] C. Tsallis, R. S. Mendes, and A. R. Plastino, "The Role of Constraints within Generalized Nonextensive Statistics," *Physica A,* vol. 261, pp. 534-554, 1998.
[31] Y. Yuan, Y. Li, and D. P. Mandic, "Comparison Analysis of Embedding Dimension between Normal and Epileptic EEG Time Series," *The Journal of Physiological Sciences,* p. 806270053, 2008.
[32] T. Gautama, D. P. Mandic, and M. M. Van Hulle, "A Differential Entropy Based Method for Determining the Optimal Embedding Parameters of a Signal," in *Acoustics, Speech, and Signal Processing Proceedings.*, 2003.
[33] J. Theiler and P. Rapp, "Re-examination of the Evidence for Low-dimensional, Nonlinear Structure in the Human EEG," *Electroenceph. Clin. Neurophysiol,* vol. 98, p. 213?22, 1996.
[34] J. Kohlmorgen, K. R. Muller, J. Rittweger, and K. Pawelzik, "Identification of nonstationary dynamics in physiological recordings," *Biological Cybernetics,* vol. 83, pp. 73-84, 2000.
[35] M. C. Mackey and L. Glass, "Oscillation and Chaos in Physiological Control Systems," *Science,* vol. 197, pp. 287-289, 1977.
[36] A. Kaplan, J. Roschke, B. Darkhovsky, and J. Fell, "Macrostructural EEG Characterization based on Nonparametric Change Point Segmentation: Application to Sleep Analysis," *Journal of Neuroscience Methods,* vol. 106, pp. 81-90, 2001.
[37] A. L. Goldberger, L. A. N. Amaral, L. Glass, J. M. Hausdorff, P. C. Ivanov, R. G. Mark, J. E. Mietus, G. B. Moody, C. K. Peng, and H. E. Stanley, "PhysioBank, PhysioToolkit, and PhysioNet Components of a New Research Resource for Complex Physiologic Signals 1." vol. 101: Am Heart Assoc, 2000.
[38] Y. Ichimaru and G. B. Moody, "Development of the Polysomnographic Database on CD-ROM," *Psychiatry and Clinical Neurosciences,* vol. 53, pp. 175-177, 1999.
[39] I. H. Song, D. S. Lee, and S. I. Kim, "Recurrence Quantification Analysis of Sleep Electoencephalogram in Sleep Apnea Syndrome in Humans," *Neuroscience Letters,* vol. 366, pp. 148-153, 2004.
[40] A. Delorme and S. Makeig, "EEGLAB: an Open Source Toolbox for Analysis of Single-trial EEG Dynamics including Independent Component Analysis," *Journal of Neuroscience Methods,* vol. 134, pp. 9-21, 2004.
[41] R. Sneddon, "The Tsallis Entropy of Natural Information," *Physica A: Statistical Mechanics and its Applications,* vol. 386, pp. 101-118, 2007.
[42] I. T. Jolliffe, *Principal component analysis*: Springer New York, 2002.
[43] R. Agarwal, J. Gotman, S. Syst, and Q. Montreal, "Computer-assisted Sleep Staging," *Biomedical Engineering, IEEE Transactions on,* vol. 48, pp. 1412-1423, 2001.
[44] P. Anderer, G. Gruber, S. Parapatics, M. Woertz, T. Miazhynskaia, G. Klosch, B. Saletu, J. Zeitlhofer, M. J. Barbanoj, and H. Danker-Hopfe, "An E-health solution for automatic sleep classification according to Rechtschaffen and Kales: validation study of the Somnolyzer 24 x 7 utilizing the Siesta database," *Neuropsychobiology,* vol. 51, pp. 115-133, 2005.
[45] J. Y. Tian and J. Q. Liu, "Automated Sleep Staging by a Hybrid System Comprising Neural Network and Fuzzy Rule-based Reasoning," *Engineering in Medicine and Biology Society, 2005. IEEE-EMBS 2005. 27th Annual International Conference of the,* pp. 4115-4118, 2005.
[46] L. Zoubek, S. Charbonnier, S. Lesecq, A. Buguet, and F. Chapotot, "Feature selection for sleep/wake stages classification using data driven methods," *Biomedical Signal Processing and Control,* vol. 2, pp. 171-179, 2007.
[47] R. G. Andrzejak, K. Lehnertz, F. Mormann, C. Rieke, P. David, and C. E. Elger, "Indications of Nonlinear Deterministic and Finite-dimensional Structures in Time Series of Brain Electrical Activity: Dependence on Recording Region and Brain State," *Physical Review E,* vol. 64, p. 61907, 2001.
[48] C. L. Ehlers, J. Havstad, D. Prichard, and J. Theiler, "Low Doses of Ethanol Reduce Evidence for Nonlinear Structure in Brain Activity," *Journal of Neuroscience,* vol. 18, pp. 7474-7486, 1998.
[49] W. S. Pritchard, D. W. Duke, and K. K. Krieble, "Dimensional Analysis of Resting Human EEG II: Surrogate-data Testing indicates Nonlinearity but not Low-dimensional Chaos," *Psychophysiology,* vol. 32, pp. 486-491, 1995.
[50] J. Jeong, M. S. Kim, and S. Y. Kim, "Test for Low-dimensional Determinism in Electroencephalograms," *Physical Review E,* vol. 60, pp. 831-837, 1999.
[51] J. M. Lee, D. J. Kim, I. Y. Kim, K. Suk Park, and S. I. Kim, "Nonlinear-analysis of Human Sleep EEG using Detrended Fluctuation Analysis," *Medical Engineering and Physics,* vol. 26, pp. 773-776, 2004.
[52] J. M. Lee, D. J. Kim, I. Y. Kim, K. S. Park, and S. I. Kim, "Detrended Fluctuation Analysis of EEG in Sleep Apnea using MIT/BIH Polysomnography Data," *Computers in Biology and Medicine,* vol. 32, pp. 37-47, 2002.
[53] M. Palus, "Nonlinearity in normal human EEG: cycles, temporal asymmetry, nonstationarity and randomness, not chaos," *Biological Cybernetics,* vol. 75, pp. 389-396, 1996.
[54] T. Banaschewski, D. Brandeis, H. Heinrich, B. Albrecht, E. Brunner, and A. Rothenberger, "Association of ADHD and conduct disorder-brain electrical evidence for the existence of a distinct subtype," *Journal of Child Psychology & Psychiatry & Allied Disciplines,* vol. 44, p. 356, 2003.
[55] D. Lehmann, P. L. Faber, S. Galderisi, W. M. Herrmann, T. Kinoshita, M. Koukkou, A. Mucci, R. D. Pascual-Marqui, N. Saito, and J. Wackermann, "EEG microstate duration and syntax in acute, medication-naive, first-episode schizophrenia: a multi-center study," *Psychiatry Research: Neuroimaging,* vol. 138, pp. 141-156, 2005.
[56] W. K. Strik, R. Chiaramonti, G. C. Muscas, M. Paganini, T. J. Mueller, A. J. Fallgatter, A. Versari, and R. Zappoli, "Decreased EEG microstate duration and anteriorisation of the brain electrical fields in mild and moderate dementia of the Alzheimer type," *Psychiatry Research: Neuroimaging,* vol. 75, pp. 183-191, 1997.
[57] B. J. Frey and D. Dueck, "Clustering by Passing Messages Between Data Points," *Science,* vol. 315, p. 972, 2007.

Charles-Francois V. Latchoumane (S'09) received the B.S. and M.S. degrees in physics and Instrumentation for biotechnologies from the Ecole Nationale Superieure de physique de Grenoble, Grenoble, France in 2004 and 2006, respectively, and the M.S. in bio and brain engineering from the Korea Advanced Institute of Science and Technology (KAIST), Deajeon, Republic of Korea in 2006.

He is currently Ph.D. candidate at the Bio and Brain Engineering Department of KAIST. His background includes signal processing, electrophysiological recordings, computational neuroscience, artificial intelligence/machine learning with application in the domain of biomedical engineering and healthcare systems (e.g. neuropathology diagnosis based on EEG including Alzheimer's disease and Attention-Deficit/Hyperactivity Disorder).

Mr. Latchoumane is also member of the International Association of Engineers (IAENG) and of the Cognitive Neuroscience Society (CNS).

Jaeseung Jeong (M'09) received the B.S., M.S., and Ph.D. in physics from the Korea Advanced Institute of Science and Technology (KAIST) in Daejeon, Republic of Korea, in 1994, 1996 and 1999, respectively.

From 1999 to 2001, he was working as a postdoc in Yale University School of Medicine, and he served a research professor (2001 - 2004) at the Department of Physics in Korea University. He was an Assistant Professor of Department of Child Psychiatry in Columbia University, College of Physicians and Surgeons (2004 - 2008), and is currently an Associate professor at the Department of Bio and Brain Engineering in KAIST since 2008. His research topics include neuroscience of decision-making, complex brain dynamics, brain-computer interface, and neuroaesthetics. He is a member of IEEE EMBS.

TABLE I

The classification accuracy (in percentage) using the linear discriminant classifier and entropy features in a leave-one-out cross-validation. The overall accuracy of each subject was estimated over the total true rate detection of all stages, and the corresponding number of sleep stages used is displayed in brackets (30 sec duration each). SWS denotes Slow Waves Sleep Stage (stages III and IV); REM denotes the Rapid Eye Movements Sleep Stage; Sens and Spec denote the sensitivity and specificity, respectively.

Classification of Sleep Stages Using the Dynamical Nonstationarity Method

Subjects	Stage I		Stage II		SWS		REM		Overall
Slp01a	Sens : 100 Spec: 95.1	(1)	Sens : 81.8 Spec: 94.1	(103)	Sens : 95.6 Spec: 95.9	(109)	Sens : 80.5 Spec: 98.6	(13)	88.5
Slp01b	Sens : 79.6 Spec: 90.6	(27)	Sens : 82.7 Spec: 873	(120)	Sens : n/a Spec: n/a	(0)	Sens : 88.0 Spec: 93.8	(25)	82.9
Slp02a	Sens : 70.0 Spec: 96.8	(18)	Sens : 81.5 Spec: 91.5	(197)	Sens : 100 Spec: 94.6	(7)	Sens : 91.4 Spec: 93.2	(77)	83.8
Slp02b	Sens : 90.9 Spec: 92.6	(14)	Sens : 87.4 Spec: 98.3	(114)	Sens : n/a Spec: n/a	(0)	Sens : 96.3% Spec: 95.7%	(29)	89.3
Slp04	Sens : 62.8 Spec: 90.7	(58)	Sens : 77.7 Spec: 82.2	(441)	Sens : 84.6 Spec: 91.9	(33)	Sens : 76.8 Spec: 96.0	(23)	76.5
Slp16	Sens : 64.9 Spec: 85.9	(108)	Sens : 75.1 Spec: 80.4	(181)	Sens : 100 Spec: 99.1	(24)	Sens : 68.3 Spec: 92.5	(65)	72.6
Slp32	Sens : 81.5 Spec: 92.1	(27)	Sens : 57.9 Spec: 80.8	(159)	Sens : 80.6 Spec: 73.3	(60)	Sens : n/a Spec: n/a	(0)	66.0
Slp37	Sens : 57.7 Spec: 95.9	(18)	Sens : 95.5 Spec: 69.8	(588)	Sens : n/a Spec: n/a	(0)	Sens : 89.1 Spec: 99.7	(11)	94.3
Slp48	Sens : 58.6 Spec: 72.7	(240)	Sens : 63.9 Spec: 71.0	(269)	Sens : 100 Spec: 96.8	(2)	Sens : 82.4 Spec: 95.5	(31)	62.8
Slp59	Sens : 62.2 Spec: 90.6	(105)	Sens : 65.8 Spec: 84.6	(94)	Sens : 91.7 Spec: 96.0	(80)	Sens : 80.9 Spec: 92.0	(35)	72.9
Slp60	Sens : 86.2 Spec: 78.4	(340)	Sens : 57.3 Spec: 88.9	(49)	Sens : n/a Spec: n/a	(0)	Sens : 70.0 Spec: 95.2	(31)	81.6
Slp61	Sens : 78.0 Spec: 87.7	(88)	Sens : 53.7 Spec: 83.7	(326)	Sens : 81.9 Spec: 86.0	(103)	Sens : 85.1 Spec: 94.9	(75)	66.2
Overall	Sens : 72.3 Spec: 89.9	(1044)	Sens : 76.2 Spec: 83.7	(2641)	Sens : 88.8 Spec: 94.9	(418)	Sens : 82.4 Spec: 95.9	(415)	77.0

TABLE II

The classification accuracy (in percentage) between different sleep stages using the linear discriminant classifier and original entropy features (Rref = 20) or the principal components corresponding to 99% of the explained variance (after PCA), in a leave-one-out cross-validation.

	Entropy Features		Principal Components	
Stage I vs. Stage II	78.7	86.2	67.5	75.3
Stage I vs. SWS	99.0	99.3	88.1	98.5
Stage I vs. REM	95.0	92.3	81.5	84.2
Stage II vs. SWS	89.2	92.7	77.7	91.5
Stage II vs. REM	94.7	88.9	78.6	83.1
SWS vs. REM	99.7	99.9	99.5	97.2

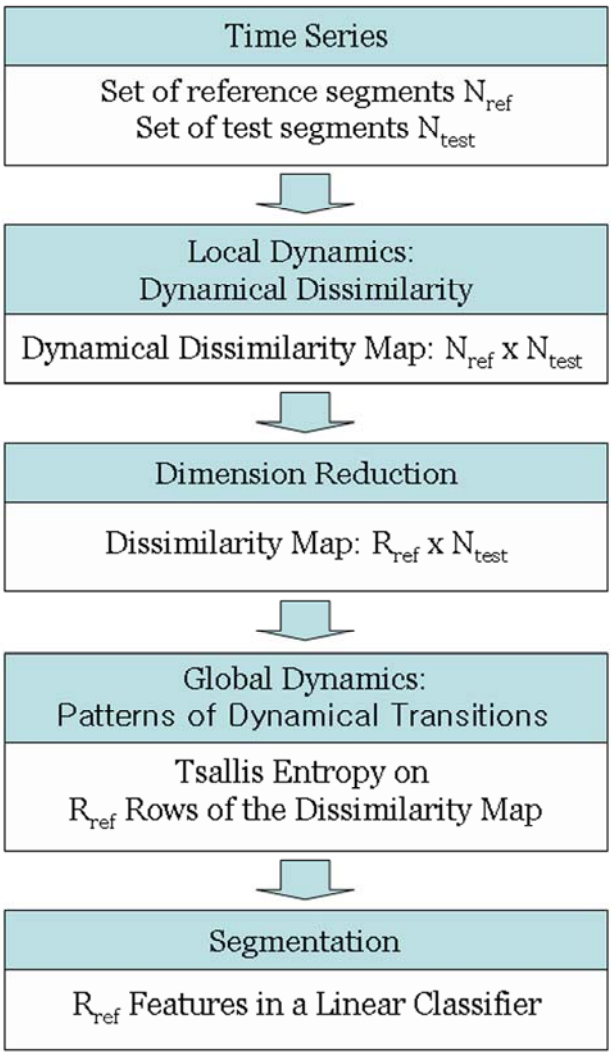

Fig. 1. Schematic diagram of dynamical nonstationarity analysis for a time series. The dynamical dissimilarity map, calculated from the phase-space dissimilarity measure (PSDM) between Nref segments and Ntest segments, is reduced to Rref × Ntest to avoid redundant features. The global dynamics or patterns of local dynamic shift of the Rref of the dissimilarity map are analyzed using the Tsallis entropy. The resulting Rref features are then fed to a linear discriminant classifier using a leave-one-out cross validation technique (also known as k-fold cross validation with k=1) to determine macrostates.

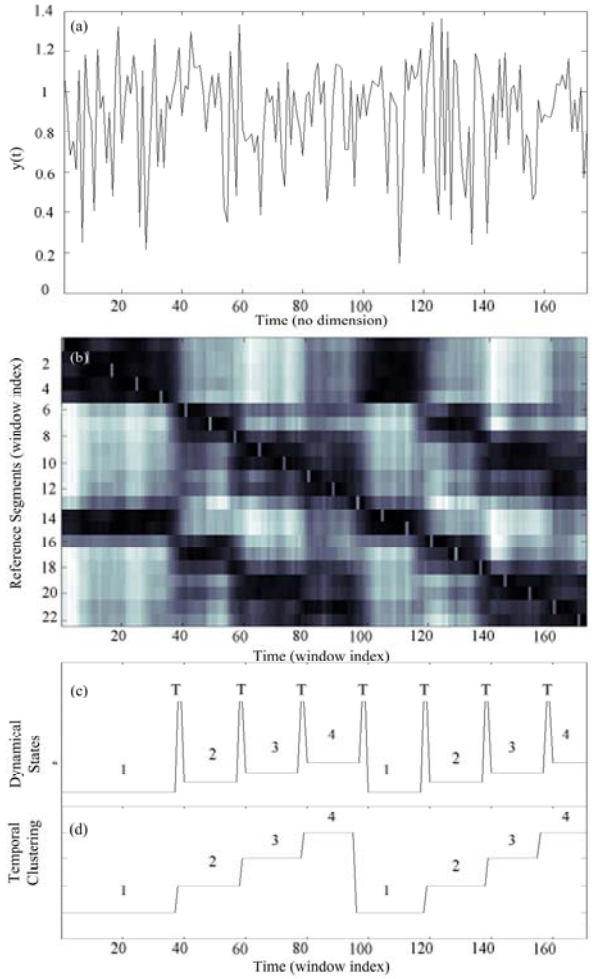

Fig. 2. Application of dynamical nonstationarity analysis to the physiological simulated time series generated from the Mackey-Glass system having four patches with exponential transition of length Dtrans = 100 points. (a) The nonstationary time series of the Mackey-Glass system resampled at $\Delta T = 25$; (b) the dynamical dissimilarity map was obtained with W = 400, OV = 350, S = 5, d = 2, and $\tau = 23$; (c) 1, 2, 3, and 4 indicate the positions of four different dynamical states, and T indicates transition timing between different dynamical states; (d) temporal clusters of the dynamical dissimilarity map using K-affinity propagation (K = 4; dashed line) and their time correspondence with the time series of the Mackey-Glass system.

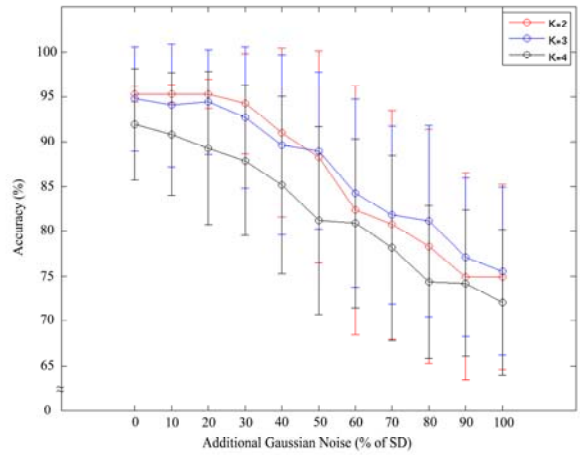

Fig. 3. Accuracy of dynamical nonstationarity analysis on the detection of different dynamical states over 100 trials: two (red), three (blue), and four (black) different dynamical states (K=2, 3, and 4). The accuracy was calculated as the ratio of true positive detections over the total number of windows. The K-affinity propagation was used to cluster dynamically stationary states from the dynamical dissimilarity map, with K set to the number of dynamics present in the time series.